Application of a Simple Buoyancy Adjustment Model to the Japan Sea*

Young-Ho SEUNG
Inha University, Inchon 402-751, Korea

Application of the simple buoyancy adjustment model, similar to Davey's (1983), indicates that buoyancies imposed locally or from outside of the basin are the major factor of the Japan Sea circulation. Within the context of the model considered, the relatively strong EW gradient of temperature, and corresponding western boundary current, in the SW region is due to the beta-effect. Kelvin waves make the western side colder and the eastern side warmer. Buoyancy input (presumably by fresh water discharge) in the NW region, so far neglected, plays an important role in strengthening the NKCC (North Korea Cold Current) and suppressing the EKWC (East Korea Warm Current) thereby breaking the conventional branching system of the Tsushima Warm Current.

Introduction

The hydrography of the Japan Sea can be generalized as follows : A very deep, cold and nearly homogeneous water (called the Japan Sea Proper Water) occupies the lower part of the basin. The upper part, much more active, can be divided into two regions, a cold sector in the N/NW and warm sector in the S/SE. Between them, a front forms though this is not always distinct. The water in the former region is fed by the Tsushima Warm Current (TWC) entering into the basin through the Korea Strait and flowing out through the straits in the NE. This region is generally characterized by relatively strong EW gradient of temperature (buoyancy) in the SW region and nearly zonal distribution far offshore (Fig. 1).

In the cold sector, the major dynamic feature is the North Korea Cold Current (NKCC) or Liman Current flowing along the western coast. A hydrographic section taken across the NW coast (e.g., Fig. 2) often shows relatively high amount of buoyancy accumulated against the coast, indicating strong southward current. As suggested by Kim and Chung (1984), and also inferred from the surface salinity distribution (Fig. 3), most of buoyancy seems to be supplied by large amount of fresh water discharge in this area. Hydrographically, this area (and further north) is characterized as the zone of cold, fresh and high oxyzen content over the whole basin (Fig. 1). Dynamically, the buoyancy input is important in carrying this water southward. This water, so transported southward by the NKCC, then affects both dynamical and hydrographical features of the warm sector. The behavior of the NKCC after reaching the edge of the warm sector is still unclear. However, one can imagine a continuation of the current along the front after leaving the coast. A fraction of the transported water which has the density exceeding that of the lowermost warm water may sink and spread beneathe the warm water along the isopycnal surfaces. This process is usually carried out by weak ageostrophic component which accompanies much stronger geostrophic component. In this regard, any transport of water which directly crosses the front seems impossible.

In observations, this water lying beneathe the warm (TWC) water corresponds to the Intermediate water named by Kajiura et al. (1958) and Moriyasu (1972) or, more precisely, to the East Sea Intermediate Water (ESIW) named by Kim and Chung (1984). The ESIW which has relatively small amount is characterized by minimum salinity and maximum oxyzen as is the NKCC water (Kim and Kim 1983).

* Contribution No. 202 of Institude of Marine Sciences, National Fisheries University of Pusan

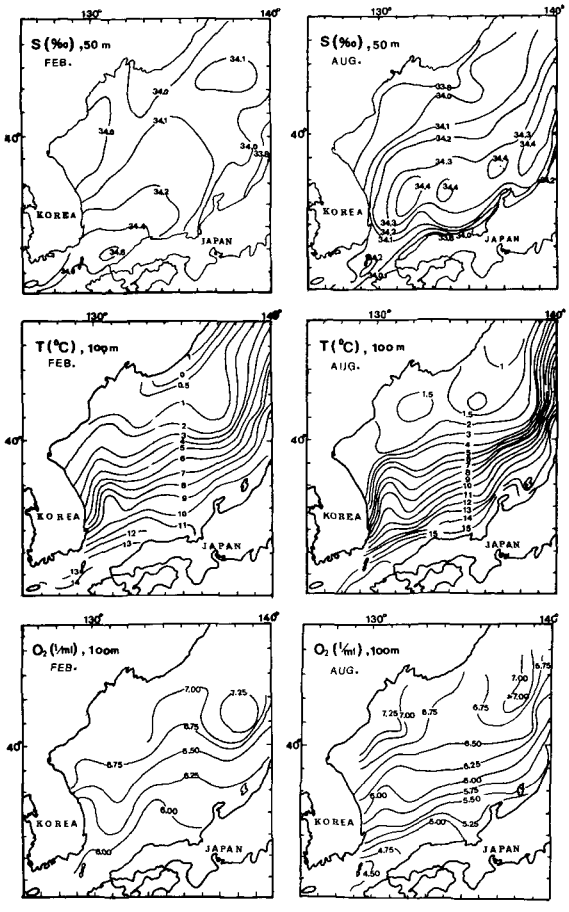

Fig. 1. Horizontal distribution of Salinity (at 100*m* depth), Temperature (at 100*m* depth) and Oxyzen content (at 100*m* depth) deduced from the historical data obtained in the Japan Sea. Data are compiled by Hydrographic Office (1982), Korea.

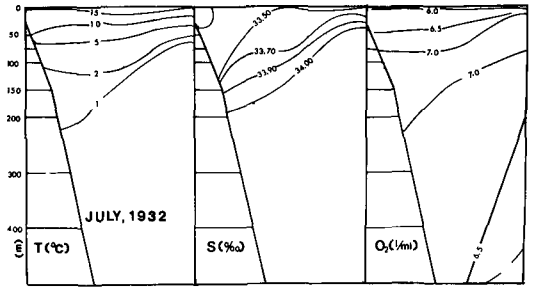

Fig. 2. The cross-shore vertical sections of Temperature, Salinity and Oxyzen content obtained by the Fishery Experiment Station in July, 1932 in the northwest (about 130°E, 42°N) of the Japan Sea. The sections extend from the coast (left) to about 90*Km* offshore.

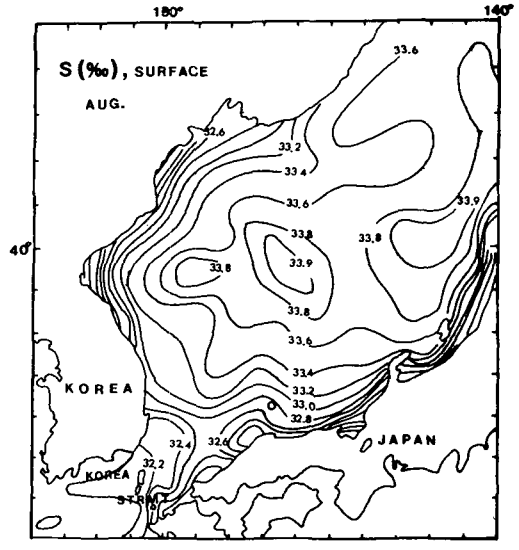

Fig. 3. Surface Salinity distribution in August in the Japan Sea. Data source is the same as Fig. 1.

This fact strongly suggests that the former is an extension of the latter. Another hypothesis about the intrusion of the ESIW, proposed by Kim and Chung (1984), is that it is transported directly from the region of formation under the guidance of bottom topography. In this regard, we cite here a study of Anderson and Killworth (1977) which shows that the bottom current in the ocean tends to be reduced by baroclinic components. Absence of bottom current automatically rules out the effect of bottom topography. In a model of low vertical resolution, such as one considered here, the motion of the ESIW will be obscured by much stronger motion of warm water lying above when averaged over the whole upper layer.

A classic view of TWC is its splitting into three branches (Suda and Hidaka, 1932 ; Uda, 1934) though Moriyasu (1972) viewed it as a meandering of one major current. Numerical experiments by Yoon (1982a, b, and c) and Kawabe (1982), where many realistic conditions are taken into consideration, succeeded to some extents in reproducing the major feature of circulation. In these studies, the nearshore branch, topographically guided and flowing northward along the Japanese coast, seems to

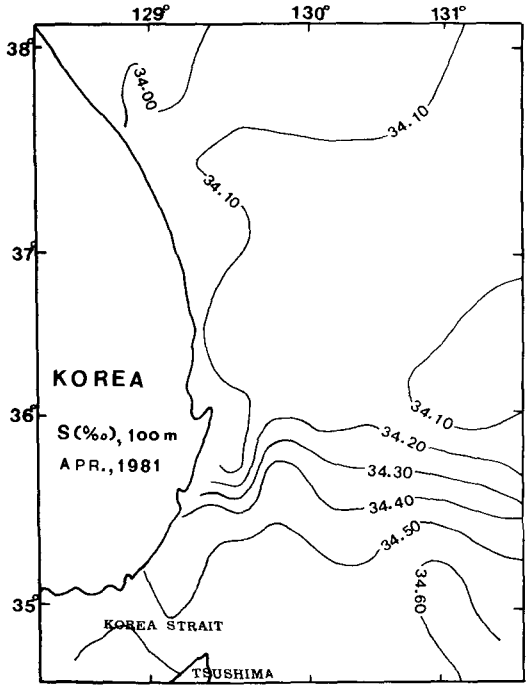

Fig. 4. Horizontal distribution of Salinity at 100*m* depth obtained by Fisheries Research and Development Agency, Korea in April, 1981.

be definite. Another branch (EKWC), flowing northward along the Korean coast, appeared as a permanent feature. There was a suggestion that this current is induced by the beta-effect and differential heating. As is often the case with complicated numerical experiments, the generation mechanism of the EKWC was not quite clear in these studies.

Furthermore, the local buoyancy input in the NW region was ignored in these studies ; this buoyancy input is very important in generating the NKCC and changing the branching system of the TWC as shown later. Concerning the latter fact, there is an important finding by Kim and Legeckis (1986). On the sattelite images, there is an occasion where the EKWC is largely suppressed southward and is not practically visible. The corresponding hydrographic data also shows a deep thermal (Kim and Legeckis, 1986, Fig. 3) and saline (Fig. 4) fronts slanting to the south. In normal conditions, two weaker fronts are expected : one in the south and another in the north, each representing two branches (Kim and Legeckis, 1986). As mentioned by these authors, this fact requires further explanations about the branching of the TWC which has been considered as a permanent feature. Accompanying this southward extension of fresh and cold water, one may expects the same southward extension of the whole NKCC system.

In this study, we try to reproduce the general circulation of the Japan Sea by using a simple buoyancy adjustment model and, more importantly, unveil the underlying mechanisms. This can be done when the problem is properly simplified though this way eliminates some details of reality. An attempt is made to answer the question how the observed temperature (buoyancy) distribution and circulation arise. Special emphasis is put on the role played by buoyancy input in the NW region which controles the strength of the NKCC and therefore affects the existence of the EKWC. The nearshore branch flowing along the Japanese coast does not appear in this model and is taken for granted. The model consiers only the steady state. However, results for a particular season can be obtained by imposing suitable conditins which can represent the season considered.

Application to the Japan Sea

Geometrically, the Japan Sea looks like a closed basin. But, dynamically, it is more like a channel because the known circulation is of inflow-outflow type rather than of closed gyre type. The lower part of the basin is topographically isolated from outsides and can be considered as a closed basin. As shown later, however, this fact can be ignored as long as the motion here remains much weaker than that in the upper layer. Effect of local wind forcing does not seem to be the major cause of the circulation. Uniform Ekman drift generated by uniform wind field in the upper mixed layer cannot change the density structure and therefore the circulation, except in narrow coastal areas ; moreover, this wind field reverses between winter and summer. This expectation of circulation is far from the known circulation pattern of the Japan Sea. For spatially varying wind field, wind stress curl determines the pressure field and therefore the circulation. In the Japan Sea, any typical wind stress curl has not been well defined. For any uniform wind stress curl (this

is a reasonable assumption considering the small size of the Japan Sea compared with the scale of atmospheric system), the classical wind-driven circulation theorem indicates uniform southward (for negative curl) or northward (for positive curl) flow in the ocean interior with some modifications along the boundaries. The observed temperature distribution (Fig. 1) and circulation inferred from it, however, exhibit a typical 'ζ' -shape which is commonly expected for the circulation driven by NS buoyancy difference (Davey, 1983 ; Ikeda, 1986). Importance of differencial thermal forcing in the Japan Sea circulation is also suggested by Yoon (1982a).

In using a simple analytic model, the ocean considered should be properly idealized in such a way that the essential part of circulation dynamics is retained. The Japan Sea is therefore largely idealized as follows : We consider a square channel (size L) with constant bottom depth H. The channel axis runs in NS with meridional boundaries ; x-axis is in zonal and y-axis is in meridional directions with origin at the SW corner. The channel is under the effect of local atmospheric thermal forcing which varies only in y-direction (a very weak benthic forcing may also present). The buoyancy of the channel will therefore always tends to adjust itself largely to this atmospheric forcing (c.f., Appedix).

Without any disturbance, complete adjustment is made. The buoyancy in this case is tentatively termed as 'eruilibrium buoyancy'. The equilibrium buoyancy at the intermediate level (the transition level between upper and lower levels in two-level system considered later) is assumed to have simple linear variation in y :

$$\phi^e = \triangle\phi(1-y/L)+\phi_c \qquad (1)$$

where : ϕ^e is the equilibrium buoyancy at the intermediate level ; $\triangle\phi$, total NS difference of it ; and ϕ_c, undisturbed buoyancy at the same level. A point source of buoyancy exists at the NW corner of the model channel. The southern opening of the model channel may be considered to represent the Korea Strait ; the northern opening, about 42° latitude line of the Japan Sea (c.f., Fig. 3). The point source at the NW corner of the model channel may represent the local bouyancy source in the NW region of the Japan Sea (c.f., Fig. 3). In this model, the buoyancy supplies along the Japanese coast (c.f., Fig. 3) are neglected. No justification is made about this. It seems, however, that moderate bouyancy supplies in this area only affect the intensity of existing current without changing the circulation pattern ; we will show later that the general feature of circulation is hardly changed by the buoyancy imposed at the SE corner of the model channel.

Under these circumstances, Davey's (1983) two-level model can be applied with slight modifications (see Appendix for details). For steady state, the linearized governing equation is expressed in terms only of the buoyancy at the intermediate level, ϕ, which also consists of ϕ_c and horizontally varying disturbances of order $\triangle\phi$:

$$\nu R^2\phi_{xxxx} - KR^2\phi_{xx} - \beta R^2\phi_x = \gamma(\phi^e - \phi) \qquad (2)$$

where : subscript x denotes differentiation with respect to x ; ν, the (lateral) eddy viscosity coefficient ; $R^2 = gH\triangle\rho/8\rho_0 f^2$, the square of Rossby radius ; g, the gravity constant ; $\triangle\rho/\rho_0$, relative value of vertical density difference between upper and lower levels in undisturbed state ; f, the Corioris' parameter ; K, the linear friction coefficient ; β, the meridional gradient of f taken constant ; $\gamma = 1/\{\delta\tau_2+(1-\delta)\tau_1\}$; $\delta = H_1/(H_1+H_2) = H_1/H$; $H_1(H_2)$, upper (lower) level thickness ; τ_1 (τ_2), the adjustment time of buoyancy at the upper (lower) level. Since the buoyancy at the upper level (ϕ_1) has much larger spatial variation than that at the lower level(ϕ_2), the distribution pattern of the former can be represented by that at the intermediate level(ϕ) which is the average of the two buoyancies, i.e., $\phi = \frac{1}{2}(\phi_1+\phi_2)$.

Meridional(y) component of motion, v, is geostrophic whereas the zonal(x) component, u, is ageostrophic due to the presence of frictional force in the meridional direction. These currents are calculated from the known buoyancy, ϕ ; see (A7) and (A 8) in Appendix. Obtained velocity is baroclinic($\vec{U}$) in terms of which currents at the upper (u_1) and lower(u_2) levels are given by

$$\vec{u}_1 = (1-\delta)\vec{U}$$
$$\vec{u}_2 = -\delta\vec{U}$$

For small δ, $\vec{U}$ can therefore represent $\vec{u}_1$ to within $O(\delta)$. As mentioned earlier, idealization of bottom topography neglects the fact that current at the

lower level is largely prevented where there is large bottom relief. This erroneous bottom current can be removed by imposing a barotropic current (not considered in this model) having the same magnitude as the bottom current but with opposite direction. In either case whether the bottom current should be removed or not, we can take $\vec{U}$ as representative of $\vec{u}_1$ to within O(δ).

As in Davey's model, boundary conditions are the conditions of no normal flow and no-slip. In applying these boundary conditions, known constant buoyancies should be imposed at the NW and SE corners (c.f., Appendix). In Davey's model, local equilibrium buoyancies are imposed at these points. For suitable use of these conditions in this study, a modification is made. Buoyancies imposed at these points are taken larger than the local equilibrium buoyancies. The reason is as follows : At the southern opening, the water advected from the south may have already been adjusted to the local atmospheric thermal forcing there, which is larger than that at the southern opening. Since the disturbances are very weak at the SE corner, the condition given from outside of the channel is retained at this point. At the NW corner, buoyancy is continuously supplied and also transported southward. In steady state, the rates of supply and transport balance each other so that the condition of constant buoyancy can be applied. These conditions are thus expressed as

$$\phi(0,\ L)=\phi^e(0,\ L)+W_N \tag{3}$$
$$\phi(L,\ 0)=\phi^e(L,\ 0)+E_S \tag{4}$$

where W_N and E_S are excesses over the local equilibrium buoyancies at the NW and SE corners, respectively. Solution of (2) and application of boundary conditions ((A17) and (A18) in Appendix), in which (3) and (4) are used, determine the whole system. In the following secions, we will consider the cases of linear friction and lateral viscosity separately to obtain an idea of the Japan Sea circulation.

Linear Friction($\nu=0,\ K\neq 0$)

For convenience, we will use the non-dimensionalized variables in the following discussions. Distance variables(x, y) are non-dimensionalized by L ; and buoyancies, ϕ and ϕ^e, by $\triangle\phi$ after subtracting ϕ_A. The solution of (2) is similar to Davey's :

$$\phi=(1-y)+W(y)\exp(-\alpha_W x)+E(y)\exp[-\alpha_E(1-x)] \tag{5}$$

where

$$\alpha_W=\frac{\beta L}{2K}+\left[\left(\frac{\beta L}{2K}\right)^2+\frac{\gamma L^2}{KR^2}\right]^{1/2}$$
$$\alpha_E=-\frac{\beta L}{2K}+\left[\left(\frac{\beta L}{2K}\right)^2+\frac{\gamma L^2}{KR^2}\right]^{1/2}$$

are inverses of westerly and easterly decay scales, respectively : W(y) and E(y) are values along the western and eastern boundaries, respectively, which are determined by applying the boundary conditions. Due to the beta-effect, the EW scale is smaller in the west than in the east.

Estimation of α_W and α_E is subject to uncertainties involved in parameter values used. In subsequent numerical evaluations, we will use the following typical values :

$L\sim 10^3$Km, $f\sim 10^{-4}$sec^{-1}, $\beta\sim 2\times 10^{-11}$ sec^{-1}m^{-1}
$K^{-1}\sim 10$day, $\gamma\sim\tau^{-1}\sim 10^{-1}$K, $H_1\sim 10^2$m
$H_2\sim 2\times 10^3$m, $\triangle\rho/\rho_0\sim 2\times 10^{-3}$

These values give $\alpha_W\simeq 25$ and $\alpha_E\simeq 5$ which means that western and eastern boundary effects decay within L/25 and L/5, respectively. For different parameter values used, α_W and α_E may vary ; for the same range of parameter values used, α_E has much narrower range of variation than α_W. However, it will be shown later that the general feature of circulation remains unchanged as long as these scales are within reasonable bounds.

The unkown functions W(y) and E(y) are determined by applying the condition of no normal flow, (A17), prescribed in Appendix. In applying the boundary condition, (3) and (4) are used instead of (A 19) ; see Appendix for details. In the case where the western boundary effect can not reach the opposite side, these are

$$W(y)=-\frac{f}{K\alpha_W}\left[1-\exp\left\{\frac{K\alpha_W}{f}(y-1)\right\}\right]\left[1-\exp(-\alpha_E)\right]+W_N\exp\left[\frac{K\alpha_W}{f}(y-1)\right] \tag{6}$$

$$E(y)=\frac{f}{K\alpha_E}\left[1-\exp\left(-\frac{K\alpha_E}{f}y\right)\right]+E_s\exp\left(-\frac{K\alpha_E}{f}y\right) \tag{7}$$

Neglect of western boundary effect on the eastern boundary means that (6) and (7) are correct to within order $\exp(-\alpha_W)$. For α_E moderately larger than unity, the multiplication factor $[1-\exp(-\alpha_E)]$ can be dropped and (6) becomes the same form as (7). In (6) and (7), the NS scale increases by a factor of about $f/K\sim100$ compared with the EW scale. In the absence of friction($K=0$), there is no NS variation along the boundaries. This is because the undamped Kelvin waves have transported the signals inposed at the NW and SE corners along the boundaries. Importance of the role played by Kelvin waves are evident here : it explains the observed EW asymmetry in hydrography(colder west and warmer east) and, as seen later, the variation of hydrography(current system) in the western side. These solution are schematized in Fig. 5 through 7 for different values of W_N. For most cases, E_S is taken constant as 0.2 but an extreme case $E_S=0.8$ is shown in Fig. 8c to emphasize that the variation of E_S is not important in changing the general feature especially in the western side ; results for different values of α_W and α_E are also shown in Fig. 8a and b to emphasize that change of scales, α_W and α_E, within reasonable bounds hardly alter the general feature.

The case of $W_N=0.2$ or 0.5 may be considered as the normal condition of the Japan Sea. In these cases, the distribution of ϕ can be compared with the observed temperature distribution (Fig. 1) except for the NW region where the buoyancy is caused by salinity. As mentioned earlier, the beta-effect renders the EW gradient stronger in the west than in the east, resulting in the western boundary current. The unit of current speed shown in these figures is $\triangle\phi/fL$. For $\triangle\phi$ about $10m^2sec^{-2}$ (this corresponds to the NS relative density difference of about 10^{-3}, see (A3) in Appendix for definition of ϕ), it becomes about 10cm/sec.

The strongest western boundary current then has speed of about 1m/sec. As the buoyancy develops at the NW corner, southward coastal current (or NKCC) strengthens and extends southward. The western boundary current (or EKWC) is then suppressed to the south and finally joins another regime which, though not appear in this model, corresponds to the alongshore branch of the TWC mentioned earlier. This change of circulation pattern can be clearly seen by examining the behavior of current along the western boundary. The alongshore current v (given by ϕ_x/f, see Appendix) reverses its sign at

$$y=1-(f/K\alpha_W)\ln[1+(K\alpha_W/f)W_N] \qquad (8)$$

This point moves southward as W_N increases, i.e., southward current (or NKCC) extends southward. The zonal current (u) has much simpler distribution by monotonically getting stronger toward the center of the basin. The southward coastal current(NKCC) returns to the north after leaving the coast forming a cyclonic circulation as suggested by Uda (1934). This northward return flow is related to the eastward pressure gradient developping outside the western boundary layer as a result of buoyancy extending from the eastern boundary.

Lateral Viscosity ($K=0$, $\nu\neq0$)

In this case, the general solution of (2) is as given by Davey :

$$\phi=(1-y)+E_1(y)\exp[\mu_1(x-1)]+E_2(y)\exp[\mu_2(x-1)]+\exp(-\mu_3x)[W_1(y)\cos\mu_4x+W_2(y)\sin\mu_4x] \qquad (9)$$

where : μ_1 through μ_4 are inverses of four length scales ; $E_1(y)$, $E_2(y)$, $W_1(y)$, and $W_2(y)$ are values along the boundaries and are determined by the boundary conditions. As in Davey's study, μ_1 is taken as the same as α_E. The other three scales, μ_2^{-1} through μ_4^{-1}, are related to the viscosity and have the same order of magnitude as the Munk's boundary layer in classical wind-driven circulation theorem. The latter scale is given by $(\nu/\beta)^{1/3}$ which is, for $\nu\sim5000m^2sec^{-1}$, about $60Km$. To obtain an idea about these scales, non-dimensionalize x by an arbitrary scale λ in (2), then determine λ by checking the balance between possible two of the three terms. We take here 20 as representative of μ_2 through μ_4, i.e., $\mu_3=\mu_4=\mu_2=20$. As mentioned previously, slight change of μ_2 through μ_4 does not alter the general feature. The unknown functions $E_1(y)$, $E_2(y)$, $W_1(y)$ and $W_2(y)$ are determined by applying boundary conditions (A17) and (A18) prescribed in Appendix. In applying these conditions, (3) and (4) are used instead of (A19) ; see Appendix for details. When boundary effects from one side to another is

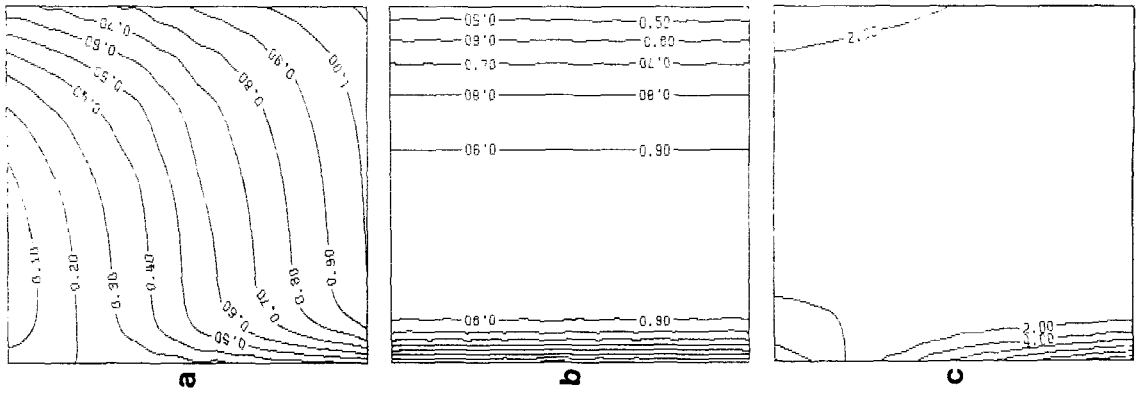

Fig. 5. Horizontal (x rightward, y upward) distribution of (a) bouyancy, (b) x-component and (c) y-component of velocity at the intermediate level obtained by solving (2) for the case of linear friction. The y-component of velocity is negative (positive) in the upper (lower) left part of the domain. Buoyancies imposed at the upper left (NW) and lower right (SE) corners are $W_N=0.2$ and $E_S=0.2$, respectively. Easterly and westerly decay scales are $\alpha_E=5$ and $\alpha_W=25$, respectively. Buoyancy and current speed are non-dimensionalized by $\triangle\phi$ and $\triangle\phi/fL$, respectively. See text for details.

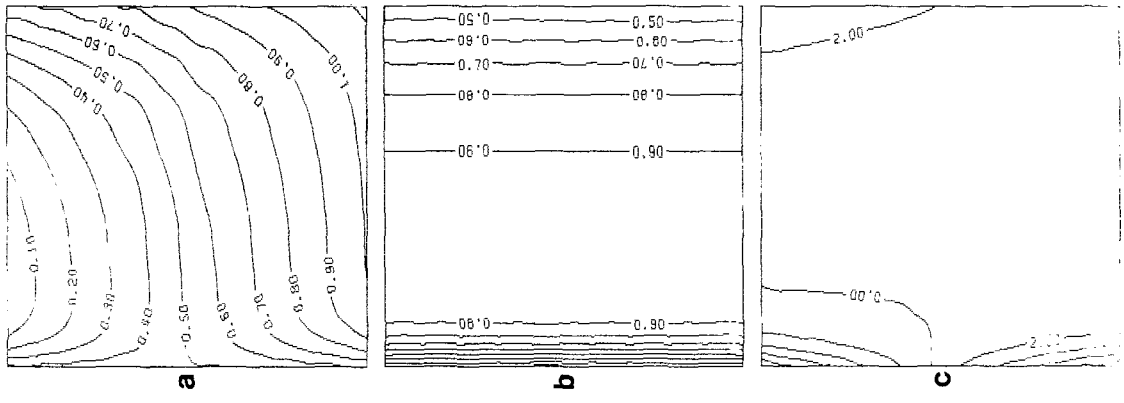

Fig. 6. same as Fig. 5 except for $E_S=0.2$ and $W_N=0.5$.

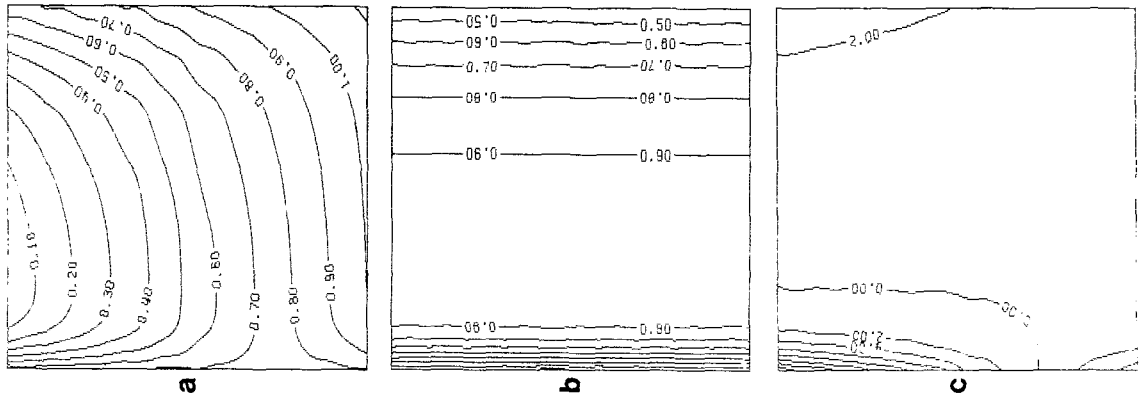

Fig. 7. same as Fig. 5 except for $E_S=0.2$ and $W_N=0.8$.

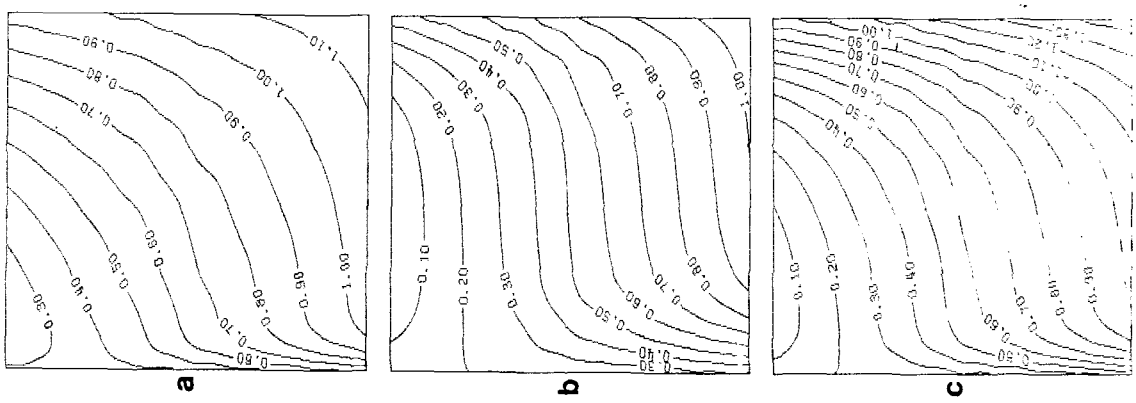

Fig. 8. Horizontal distributions of buoyancy at the intermediate level : (a), for $\alpha_E=2$, $\alpha_W=40$ and $E_S=W_N=0.2$; (b), for $\alpha_E=8$, $\alpha_W=10$ and $E_S=W_N=0.2$; and (c), for $\alpha_E=5$, $\alpha_W=25$, $E_S=0.8$ and $W_N=0.2$. All others are the same as Fig. 5.

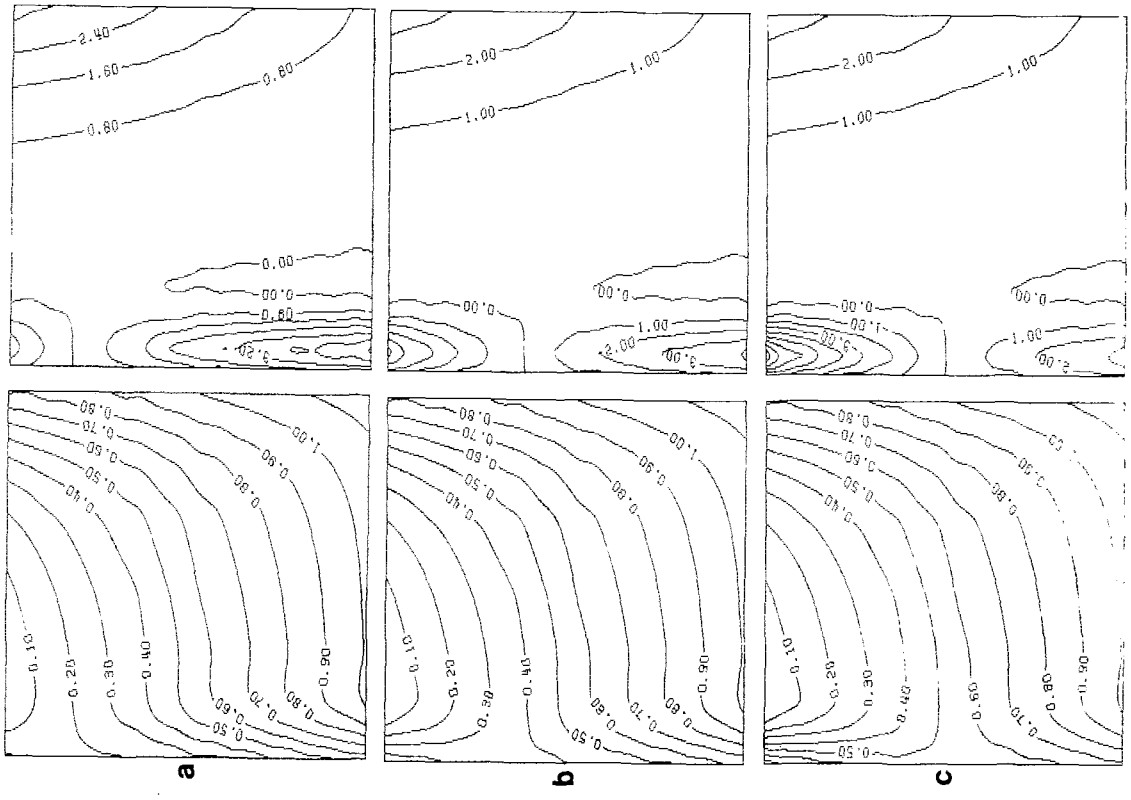

Fig. 9. Horizontal distribution of buoyancy (left panel) and y-component of velocity (right panel) at the intermediate level obtained by solving (2) for the case of lateral eddy viscosity : (a), for $E_S=W_N=0.2$: (b), for $E_S=0.2$ and $W_N=0.5$; and (c), for $E_S=0.2$ and $W_N=0.8$. In all cases, the decay scales are $\mu_1=5$ and $\mu_2=20$. The y-component of velocity is negative in the upper left part of the domain and just right side of the western boundary current. All others are the same as Fig. 5. See text for more details.

neglected (i.e., to within order $\exp(-\mu_1)$), these functions are

$$E_1(y)=\{1-\exp(-A_1y)\}/A_1(1-\mu_1/\mu_2)+E_S\exp(-A_1y)/(1-\mu_1/\mu_2) \quad (10)$$

$$E_2(y)=-\mu_1E_1/\mu_2 \quad (11)$$

$$W_1(y)=-\{1-\exp\{A_2(y-1)\}\}/A_2-W_N\exp\{A_2(y-1)\} \quad (12)$$

$$W_2(y)=W_1(y) \quad (13)$$

where A_1 and A_2 are the inverses of NS scale along the eastern and western boundaries, respectively, given by

$$A_1=\nu\mu_2^2\mu_1/fL^2,\ A_2=4\nu\mu_1\mu_2^2/fL^2$$

For parameter values given earlier, the NS scales are larger than the corresponding EW scales by a factor of order 100, same as that in the case of linear friction. Without viscosity ($A_1=A_2=0$), these scales become infinitely large and the same discussions can be made about the role of Kelvin waves as before. The results (Fig. 9a through c) show basically the same feature as that in the case of linear friction. The only differences are : the maximum v occurs somewhat offshore (at $x=x_{max}$) ; weak counter current develops beside the western boundary current ; and the development of southward current with W_N is somewhat slower than that in the case of linear friction. In the same way as before, the change of circulation pattern in the west can be seen by examining v along the line $x=x_{max}$. The current reversal occurs at point.

$$y=1-ln\{1+A_2W_N\}/A_2 \quad (14)$$

This point moves southward as W_N increases.

Concluding Remarks

A simple buoyancy adjustment model, similar to Davey's (1983), applied to the Japan Sea reproduces well the general feature of circulation. The results indicate that the buoyancies imposed locally or from outsides of the basin are the major factors of the Japan Sea circulation. Propagation of Kelvin waves makes the western side colder and the eastern side warmer resulting in cyclonic tilt of the front between warm and cold sectors which, otherwise, is zonal. Within the context of the model considered, the beta-effect makes a relevively strong EW temperature gradient in the SW region. The western boundary current forms, therefore, in this region. An important finding is that the buoyancy input in the NW region, so far neglected, plays a critical role in controling the hydrography (and therefore the current system) of the western basin. This buoyancy input (presumably by fresh water discharge) strengthens the NKCC flowing southward along the coast. This current system and accompanying hydrographic regime then extends southward. In the extreme case such as that observed by Kim and Legeckis (1986), the EKWC (western boundary current) is largely suppressed to the south and finally joins the alongshore branch of the TWC flowing northward along the Japanese coast. In future modeling of the Japan Sea circulation, this buoyancy input in the NW region should therefore be included. Further refined results can be obtained through numerical methods in which more realistic conditions are imposed such as the geometry of basin and buoyancy fluxes (by including diffusion terms) along the coast.

The model considered here resolves only the lowest baroclinic mode. Here, the upper level is occupied either by cold water or by warm water. Actually, the former intrudes beneathe the latter thereby forming the ESIW (cold, fresh and high oxyzen water) which reaches far to the bottom of the Korea Strait. This process may be resolved by constructing a model in which the thermo-haline effect and vertical convection are taken into account. Although the effect of local wind is not the major factor of the Japan Sea circulation, advection of buoyancy can occur by the wind. It should therefore be analysed to what extent the wind modifies the circulation. For completeness, non-linear effect should also be considered though it does not seem to alter the general feature (c.f., Davey, 1983).

Acknowledgements

This work is partly funded by '87 research support programs of Ministry of Education. The support is made through the Institute of Marine Sciences, Pusan Fisheries College.

Appendix

The basic concept of Davey's model is the generation of large-scale circulation by the adjustment of buoyancy. Presence of meridional boundaries (the ocean is assumed as a channel running in NS) is the crucial factor in inducing the circulation by redistributing the buoyancy which, otherwise, exhibits zonal distribution under the effect of local atmospheric (with weak benthic) thermal forcing. Two level model is employed in which the ocean column is represented simply by upper and lower levels. Buoyancy equations at two levels are

$$\phi_{1t}+\nabla\cdot(\vec{u}_1\phi_1)-W_1\phi_1/H_1=F_1 \qquad (A1)$$
$$\phi_{2t}+\nabla\cdot(\vec{u}_2\phi_2)+W_1\phi_1/H_2=F_2 \qquad (A2)$$

where : suscript means time derivative ; ϕ_i (i=1, 2), the buoyancy at ith level ; u_i, (horizontal) velocity vector at ith level ; W_1, vertical velocity at intermediate level ; ϕ_1, buoyancy at intermediate level ; H_i, the thickness of ith level ; F_i, virtual buoyancy forcing at ith level. At any level considered, the buoyancy, ϕ, is defined in terms of density, ρ, as follows :

$$\phi-\phi_0=-(gH/2)(\rho-\rho_0)/\rho_0 \qquad (A3)$$

where : ϕ_0 and ρ_0 are reference scales ; $H=H_1+H_2$; and g, the gravity constant. The virtual buoyncy forcing, F_i, is simply parameterized as

$$F_i=(\phi_i^e-\phi_i)/\tau_i \qquad (A4)$$

where ϕ_i^e is the buoyancy adjusted to the local atmospheric (or benthic) thermal forcing and τ_i is the buoyancy adjustment time, both at ith level. Expression in (A4) means that buoyancy, ϕ_i, always tends to restore to ϕ_i^e within time scale τ_i. This tendancy is taken as proportional to the deviation, $\phi_i^e-\phi_i$. The buoyancy at the intermediate level ϕ_1 (abbreviated to ϕ hereafter) is defined by

$$\phi=\frac{1}{2}(\phi_1+\phi_2) \qquad (A5)$$

The vertical velocity at the intermediate level, W_1, is related to the (horizontal) divergence of baroclinic current $\vec{U}$ (only baroclinic component appears here) as follow :

$$W_1=(1-\delta)\delta H\nabla\cdot\vec{U} \qquad (A6)$$

where $\delta=H_1/H$.

Linear momentum equations are used where the NS(y) component of current is taken geostrophic. Due to the boundary effects, ageostrophy is retained in NS momentum balance, i.e., the EW(x) component of current is ageostrophic. Thanks to the two-level approximation, the vertical shear of current, $\vec{U}=(u, v)$, is easily related to the horizontal variation of buoyancy at the intermediate level :

$$fv=\phi_x \qquad (A7)$$
$$v_t+fu=-\phi_y-Kv+\nu v_{xx} \qquad (A8)$$

where : f is the Coriolis' parameter ; subscripts x and y, differentiations with respect to x and y, respectively ; K, coefficient of linear friction ; ν, (lateral) eddy viscosity coefficient.

In steady state, the buoyancy equations, (A1) and (A2), give

$$\phi_x=\phi_x^e-B_2(\phi-\phi^e)-B_3\vec{U}\cdot\nabla\phi \qquad (A9)$$
$$\frac{1}{2}\nabla(\vec{U}\phi_x)-\frac{B_2}{2}\vec{U}\cdot\nabla\phi+\gamma(\phi-\phi^e)=0 \qquad (A10)$$

where : $\phi_x=(\phi_1-\phi_2)/2$; $\phi_x^e=(\phi_1^e-\phi_2^e)/2$; $\phi^e=(\phi_1^e+\phi_2^e)/2$; $\gamma=1/[\delta\tau_2+(1-\delta)\tau_1]$; $B_2=[\delta\tau_2-(1-\delta)\tau_1]/$; $B_3=2\delta(1-\delta)\tau_1\tau_2/\gamma$.

For more detailed derivation, refer to Davey (1983). Substitution of (A9) into (A10) eliminates ϕ_x. For small disturbances, linearization is made by omitting $\vec{U}\cdot\nabla\phi$ and setting $\phi_x=\phi_x^e$. The horizontal divergence $\nabla\cdot\vec{U}$ appearing in this process is easily expressed in terms of ϕ alone using (A7) and (A8). The resulting governing equation is

$$\nu d^2\phi_{xxxx}-Kd^2\phi_{xx}-a\phi_x=\gamma(\phi^e-\phi) \qquad (A11)$$

where : $d^2=\phi_x^e/2f^2$ is the square of Rossby radius for local stratification, ϕ_x^e ; $a=\beta d^2(1+B_1)$; β ; meridional gradient of f taken as constant ; $B_1=-(\phi_x^e+B_2\phi^e)_y f/\beta\phi_x^e$.

In the linearization above, ϕ_x is taken approximately as ϕ_x^e. Since B_2 is of O(1), this means that, in (A9), ϕ and ϕ^e have the same order of magnitude. In obtaining (A11) from (A10), however, $\vec{U}\cdot\nabla\phi$ is neglected whereas $\vec{U}\cdot\nabla\phi^e$ is not. This seems to be a contradiction. A slight modification of assumption can remove this contradiction and, moreover, allows to obtain a simpler equation. Assume that

$$\phi_i = \phi_{ci} + \phi'_i \quad \text{(A12)}$$

$$\phi^c_i = \phi_{ci} + \phi^{c\prime}_i \quad \text{(A13)}$$

where : ϕ_{ci} is the undisturbed, basic-state buoyancy at ith level varying only vertically ; ϕ'_i is the small disturbance which the buoyancy finally has at ith level ; and $\phi^{c\prime}_i$ is the small disturbance arising from the adjustment of ith level to the local atmospheric (or benthic) thermal forcing alone. For convenience, the reference scale, ϕ_0, is dropped in (A12) and (A 13) ; or it can be thought that ϕ_{ci} comprises ϕ_0. All primed buoyancies and $\vec{U}$ have first order magnitudes whereas ϕ_{ci} has zeroth order magnitude. The definition of ϕ_i with the use of (A12), then gives

$$\phi_i = \frac{1}{2}(\phi_{c1} + \phi_{c2}) + \text{first order terms} \quad \text{(A14)}$$

Whereas, (A9) reduces to the first order balance when (A12) and (A13) are substituted into it. Substituting (A14) into (A10) leads to the final first order balance :

$$\frac{1}{2}(\phi_{c1} - \phi_{c2})\nabla \cdot U = \gamma(\phi^c - \phi) \quad \text{(A15)}$$

Substituting again the expression for the horizontal divergence (obtained from the momentum equations) into (A15) leads to the governing equation :

$$\nu R^2 \phi_{xxxx} - KR^2 \phi_{xx} - \beta R^2 \phi_x = \gamma(\phi^c - \phi) \quad \text{(A16)}$$

where, at this time, all coefficients are constant ; the Rossby radius R is given by $R^2 = (\phi_{c1} - \phi_{c2})/4f^2$ which, in terms of density, is equivalent to $R^2 = gH \Delta\rho / 8\rho_0 f^2$ where $\Delta\rho/\rho_0$ is the relative value of vertical density difference between upper and lower levels in undisturbed state.

Boundary conditions are the condition of no normal flow($u=0$) and no-slip condition ($v=0$) along the boundaries. For steady state, these are given from (A7) and (A8) as

$$\phi_x + K\phi_x/f - \nu\phi_{xxx}/f = 0 \quad \text{along the} \quad \text{(A17)}$$

$$\phi_x = 0 \ (\text{only for } \nu \neq 0) \quad \text{boundaries} \quad \text{(A18)}$$

The condition (A17) involves first order differential equation with respect to y and one boundary condition is needed at the end of each boundary. The condition of constant buoyancy is thus imposed at the NW and SE corners of the ocean considered where the buoyancies are expected to remain adjusted to the local atmospheric (or benthic) thermal forcing ; disturbances are very weak at these points. These conditions are

$$\phi = \phi^c \text{ at NW and SE corners} \quad \text{(A19)}$$

These conditions, (A19), are later modified for suitable use in the problem considered.

References

Anderson, D. L. T. and P. D. Killworth. 1977. Spin-up of a stratified ocean with topography. Deep-Sea Res. 23, 709~732.

Davey, M. K. 1983. A two-level model of a thermally forced ocean basin. J. Phys. Oceanogr. 13, 169~190.

Hydrographic Office. 1982. Marine Environmental Atlas of Korean Waters. Pub. No. 1451. Nov. 1982.

Ikeda, M. 1986. Density-driven general circulation in a closed basin using a two-level model. J. Phys. Oceanogr. 16, 902~918.

Kajiura, K., M. Tsuchiya and K. Hidaka. 1958. The analysis of oceanographical condition in the Japan Sea (in Japanese). Rep. Develop. Fish. Resour. in : The Tsushima Warm Current, 1, 158~170.

Kawabe, M. 1982. Branching of the Tsushima Warm Current in the Japan Sea, Part II. Numerical experiment. J. Oceanogr. Soc. Japan 38, 97~107.

Kim, C. H. and K. Kim. 1983. Characteristics and origin of the cold water mass along the east coast of Korea (in Korean). J. Oceanol. Soc. Korea 18, 73~83.

Kim, K. and J. Y. Chung. 1984. On the salinity-minimum and dissolved oxygen-maximum layer in the East Sea (Sea of Japan). in : Ocean Hydrodynamics of the Japan and East China Seas, T. Ichiye, ed., Elsevier Science Pub., Amsterdam, 55~65.

_____ and R. Legeckis. 1986. Branching of the Tsushima Current in 1981~1983. Prog. Oceanogr. 17, 265~276.

Moriyasu, S. 1972. The Tsushima Current. in : Kuroshio, H. Stommel and K. Yoshida, ed., Univ.

of Washington Press, 353~369.

Suda, K. and K. Hidaka. 1932. The results of oceanographical observations on board R. M. S. Syunpu Maru in the southern part of the Japan Sea in the summer of 1929, Part I (in Japanese). J. Oceanogr. 3, 291~375.

Uda, M. 1934. The results of simultaneous oceanographical investigations in the Japan Sea and its adjacent waters in May and June, 1932 (in Japanese). J. Imper. Fish. Exper. St. 5, 57~190.

Yoon, J. H. 1982a. Numerical experiment on the circulation in the Japan Sea, Part I. Formation of the East Korean Warm Current. J. Oceanogr. Soc. Japan 38, 43~51.

_____, 1982b. Numerical experiment on the circulation in the Japan Sea, Part II. Influence of seasonal variation in atmospheric conditions on the Tsushima Current. J. Oceanogr. Soc. Japan 38, 81~94.

_____, 1982c. Numerical experiment on the circulation in the Japan sea, Part III. Formation of the nearshore branch of the Tsushima Current. J. Oceanogr. Soc. Japan 38, 119~124.

Received June 10, 1988
Accepted August 29, 1988